PERGAMON

International Journal of Heat and Mass Transfer 45 (2002) 3313–3320

International Journal of HEAT and MASS TRANSFER

www.elsevier.com/locate/ijhmt

Combined 'flow and strength' geometric optimization: internal structure in a vertical insulating wall with air cavities and prescribed strength

S. Lorente [a], A. Bejan [b,*]

[a] Department of Civil Engineering, National Institute of Applied Sciences (INSA), 135 Avenue de Rangueil, Toulouse 31077, France
[b] Department of Mechanical Engineering and Materials Science, Duke University, Box 90300, Durham, NC 27708-0300, USA

Received 24 August 2001; received in revised form 25 January 2002

Abstract

This paper addresses the fundamental problem of optimizing the internal structure of a vertical wall that must meet two requirements, thermal insulation and mechanical strength. The wall is a composite of solid material (e.g., brick) and parallel air caverns with varying thickness and number. It is shown that the internal structure of the wall (the number of air caverns) can be optimized so that the overall thermal resistance of the wall is maximal, while the mechanical stiffness of the wall is fixed. The maximized thermal resistance increases when the effect of natural convection in the air gaps is weaker, and when the specified wall stiffness decreases. The optimal number of air gaps is larger when the effect of natural convection is stronger, and when the specified wall stiffness is smaller. The optimal structure is such that the volume fraction occupied by air spaces decreases when the natural convection effect (the overall Rayleigh number) increases, and when the prescribed wall stiffness increases. The paper draws attention to a new class of thermal design problems, in which the system architecture is derived from a combination of heat transfer and mechanical strength considerations. This class represents an extension of the constructal design method, which until now has been used for maximizing thermofluid performance subject to size constraints. © 2002 Elsevier Science Ltd. All rights reserved.

Keywords: Constructal design; Topology; Configuration; Optimization; Thermal resistance; Insulation; Stiffness; Rigidity; Strength of materials

1. Flow system geometry: variable and optimized, not frozen

In this paper we draw attention to the close relationship between the internal structure of a flow system and its global thermal performance [1–3]. The fundamental question that we address is how to select the size of air cavities in walls or wall elements (e.g., bricks) for the purpose of maximizing the global resistance to heat transfer through the wall. We propose this fundamental problem on the background of a large volume of published research on heat transfer through specified (frozen) enclosure configurations that are heated from one side and cooled from the other. This body of published work is not reviewed here. It is summarized for example in [4–8]: its main results are accepted and used in the present study, e.g., Eq. (17).

The problem we consider is fundamentally different: it is about the optimization of geometry for a specific purpose, in this case, the maximization of the global performance of the side-heated wall with internal air cavities. It is about the optimization of the topology of a potentially complex flow system, in accordance with the main thread of constructal design and theory [3].

The design opportunity for varying and optimizing the geometric form of cavities in walls with natural

* Corresponding author. Tel.: +1-919-660-5309; fax: +1-919-660-8963.
E-mail address: dalford@duke.edu (A. Bejan).

0017-9310/02/$ - see front matter © 2002 Elsevier Science Ltd. All rights reserved.
PII: S0017-9310(02)00052-2

Nomenclature

b	dimensionless group, Eq. (20)
g	gravitational acceleration, m s^{-2}
H	height, m
I	area moment of inertia, m^4
$\tilde{I}$	dimensionless area moment of inertia, Eq. (10)
k	thermal conductivity, W m^{-1} K^{-1}
L	overall thickness, m
m	exponent, Eq. (18)
n	number of air gaps
Nu	Nusselt number, Eq. (16)
R	overall thermal resistance, W K^{-1}
$\tilde{R}$	dimensionless thermal resistance, Eq. (19)
Ra	Rayleigh number, Eq. (6)
t	thickness, m
W	wall width, m
x	transversal coordinate, m

Greek symbols

α	thermal diffusivity, m^2 s^{-1}
β	coefficient of volumetric thermal expansion, K^{-1}
ΔT	overall temperature difference, K
θ	temperature difference across one air gap, K
ν	kinematic viscosity, m^2 s^{-1}
ϕ	air volume fraction

Subscripts

a	air
b	solid
c	critical
max	maximum
opt	optimum
0	reference

convection was recognized in a few previous studies, e.g., [1,2,9,10]. The global objective in those studies, however, was the minimization of the thermal resistance of the fluid-filled cavity alone, not the maximization of the insulation capability of an assembly of cavities and separating walls (the present problem). For example, it was shown that for two-dimensional natural convection in a vertical cavity with side-to-side heat transfer the global resistance is minimum when the aspect ratio of the cavity has a value of order 1 or smaller, the smaller when the Rayleigh number is larger [8,9]. In other words, the heat transfer across the cavity is impeded the least when the cavity shape is relatively 'round', i.e., close to square. The same conclusion was reached in a more recent study by Frederick [10].

Lorente [1] and Lartigue et al. [2] have documented the behavior of the global resistance when the side walls of the cavity are deformed (bowed inward) so that the cavity profile resembles a concave lens. Deformations of this kind are commonly found in the air cavities between two glass panes in cold and windy climates. These studies showed that the global resistance to heat transfer increases significantly, this, in spite of the fact that the narrowing of the cavity mid-section suppresses the flow and its natural convection effect.

Even though the few existing studies have dealt with the minimization of the global thermal resistance, they are important because they document the strong relationship that exists between global performance and cavity geometry. This is the relationship that we exploit in the present paper. Our objective is the optimization of the wall with internal cavities as an insulation system that must also perform adequately as a strong mechanical structure.

2. The competition between thermal and mechanical objectives

Why should we expect to find an optimal cavity size when we design a cavernous wall as an insulation system? Consider the two-dimensional wall configuration shown in Fig. 1. Its overall dimensions are fixed – the

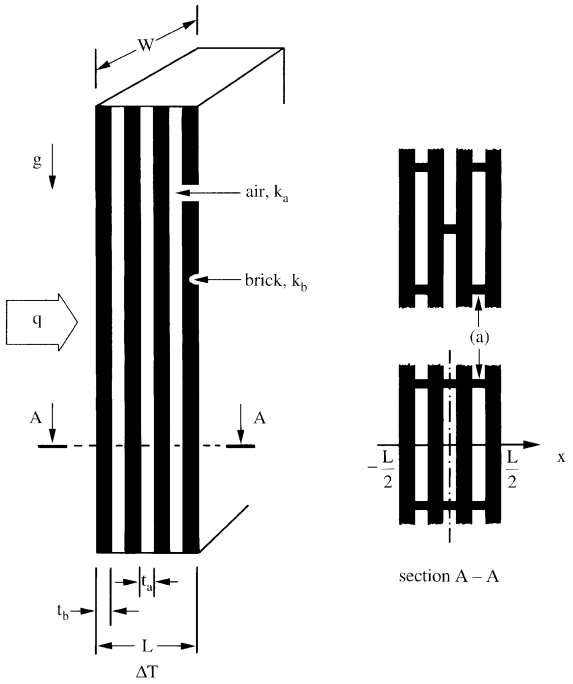

Fig. 1. Vertical insulating wall with alternating layers of solid (brick) material and air.

thickness L, the height H, and the width W perpendicular to the plane of Fig. 1. There are n vertical air-filled cavities of thickness t_a, which are distributed equidistantly over the wall thickness L. This means that there are $(n+1)$ slabs of solid wall material (e.g., brick) of individual thickness t_b, which are also distributed equidistantly. We characterize the air and brick (terra cotta) composite by using the air volume fraction ϕ, which along with the wall volume HLW is a global design parameter

$$\phi = nt_a/L, \tag{1}$$

$$1-\phi = (n+1)t_b/L. \tag{2}$$

The overall thermal resistance of this composite is the sum of the resistances of air and brick layers. If the heat transfer across each air space is by pure conduction, then the thermal resistance posed by each air space is $t_a/(k_aHW)$, where k_a is the thermal conductivity of air. Similarly, the resistance of each layer of brick material is $t_b/(k_bHW)$. The overall resistance is

$$R = \frac{nt_a}{k_aHW} + \frac{(n+1)t_b}{k_bHW} \tag{3}$$

or, after using Eqs. (1) and (2),

$$R = \frac{\phi L}{k_aHW} + \frac{(1-\phi)L}{k_bHW}. \tag{4}$$

Eq. (4) states that the thermal performance of the composite does not depend on the varying geometry, i.e., on how many air spaces and slabs of brick we use. This is correct, but only when the air space is ruled by pure conduction, i.e., when the thickness t_a is smaller than the thickness of the laminar natural convection boundary layers that would line the vertical walls of each cavity. The order of magnitude criterion for small t_a must be [8]

$$t_a \lesssim HRa_{H,\theta}^{-1/4}, \tag{5}$$

where $Ra_{H,\theta}$ is the Rayleigh number based on the height (H) and temperature difference (θ) across one air cavity

$$Ra_{H,\theta} = g\beta H^3\theta/(\alpha\nu). \tag{6}$$

The temperature difference θ is smaller than the overall temperature difference ΔT that is maintained across the entire system (Fig. 1). In the case of air and brick material, the two thermal conductivities are markedly different ($k_b/k_a \sim 20 \gg 1$), and this means that the overall ΔT is essentially the sum of the temperature differences across all the air cavities

$$\Delta T \cong n\theta. \tag{7}$$

Putting Eqs. (5)–(7) together, we see that the insensitivity of R to varying the internal structure (n), Eq. (4), can be expected only when the number of air spaces is large enough,

$$n^{5/4} \gtrsim \phi\frac{L}{H}Ra_{H,\Delta T}^{1/4}. \tag{8}$$

In this inequality, $Ra_{H,\Delta T}$ is based on the overall temperature difference, $Ra_{H,\Delta T} = g\beta H^3\Delta T/(\alpha\nu)$, and is a known constant because H and ΔT are specified global parameters.

If the number of air spaces is smaller than in Eq. (8), the natural convection effect decreases the resistance posed by each air space, and the overall R value is greater than in Eq. (3). This is why a large enough n, or a small enough t_a, is desirable from a thermal insulation standpoint. On the other hand, the effect of a large n is detrimental to the mechanical stiffness (rigidity) of the wall assembly. When ϕ is prescribed, the stiffest assembly is the one where all the solid material is placed in the outermost planes, i.e., the wall where two t_b-thin slabs sandwich a single air space. The stiffest wall is the worst thermal insulator, because it contains the thickest air space, which is penetrated by the largest natural convection heat transfer current. The optimal internal structure of the wall (n) results from the competition between thermal performance and mechanical performance. If the mechanical performance is specified, then the wall stiffness serves as constraint in the process of maximizing thermal performance, from which the optimal geometric form emerges.

3. Stiffness

The mechanical strength of the wall, or its resistance to bending and buckling in the plane of Fig. 1 is controlled by the area moment of inertia of the horizontal wall cross-section [11,12]

$$I_n = \int_{-L/2}^{L/2} x^2 W\,\mathrm{d}x. \tag{9}$$

The cross-section over which this integral is performed, is sketched in the details shown on the right-hand side of Fig. 1. The area element $W\ \mathrm{d}x$ counts only the solid parts of the cross-section, namely, the t_b-thick slabs of brick material. For the sake of simplicity, in this calculation we neglect the transversal ribs [see detail (a) in Fig. 1] that connect the t_b slabs so that the wall cross-section rotates as a plane during pure bending. We assume that the transversal ribs use considerably less material than the t_b slabs. Their role is the same as the role of the central part (the web) of the I profile of an I-beam. In fact, the cross-section of the cavernous wall structure is a conglomerate of I-beam profiles that have been fused solidly over the top and bottom surfaces of the I shape. In practice, the ribs (a) are more commonly arranged in a staggered pattern, as shown in the upper-right corner of Fig. 1.

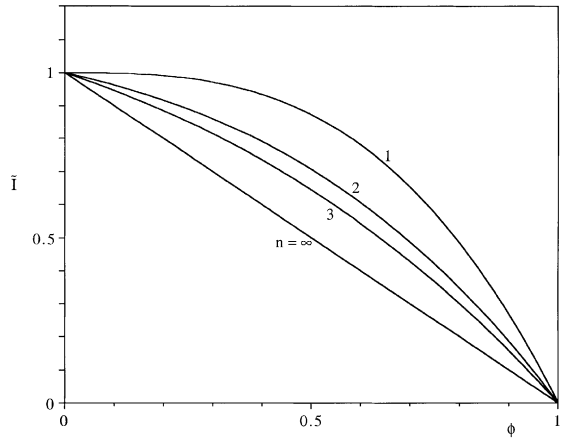

Fig. 2. The area moment of inertia of the wall cross-section, as a function of the number of air gaps and air volume fraction.

In the case of a wall with vanishing cavities ($\phi = 0$) the area moment of inertia is maximum and equal to $L^3W/12$. We use this value as reference in the nondimensionalization of I_n,

$$\tilde{I}_n = \frac{I_n}{L^3W/12}, \tag{10}$$

where the subscript n indicates the number of air gaps. We evaluate integral (9) case by case, assuming in each case that the cross-section is symmetric about $x = 0$,

$$\tilde{I}_1 = 1 - \phi^3, \tag{11}$$

$$\tilde{I}_2 = 1 + \left(\frac{1-\phi}{3}\right)^3 - \left(\frac{1+2\phi}{3}\right)^3, \tag{12}$$

$$\tilde{I}_3 = 1 + \left(\frac{3-\phi}{6}\right)^3 - \left(\frac{\phi}{3}\right)^3 - \left(\frac{\phi+1}{2}\right)^3, \tag{13}$$

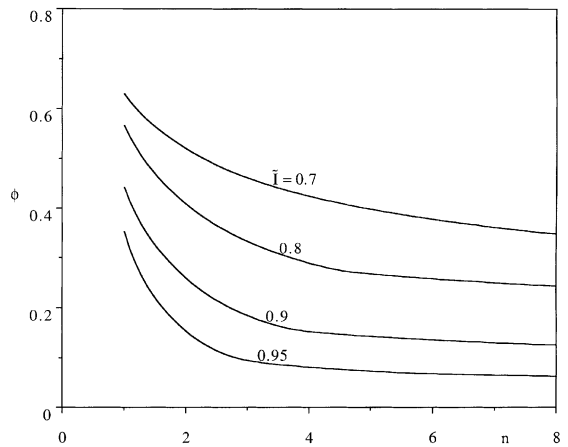

Fig. 3. The relation between air volume fraction and number of air gaps when the area moment of inertia of the wall cross-section is constrained.

$$\tilde{I}_\infty = 1 - \phi. \tag{14}$$

These results are displayed in Fig. 2. The stiffness is larger when n and ϕ are smaller.

An alternative view of this relation is presented in Fig. 3. When the stiffness is constrained, $\tilde{I}_n = \text{constant}$, for each geometry ($n$) that the designer might contemplate there is one value of ϕ that the wall composite must have. In such cases the ϕ value is larger when the number of air gaps is smaller. Less structural (solid) material is needed when there are fewer air gaps.

4. Thermal resistance

When the effect of natural convection cannot be neglected, the overall thermal resistance formula (3) has the form

$$R = \frac{nt_a}{k_a HWNu} + \frac{(n+1)t_b}{k_b HW}. \tag{15}$$

In the denominator of the first term (the contribution of all the air gaps), Nu is the overall Nusselt number that expresses the relative heat transfer augmentation effect due to natural convection in a single air space,

$$Nu = \frac{q_{\text{actual}}}{q_{\text{conduction}}}. \tag{16}$$

Several correlations of experimental and numerical Nu values have been reported [13–23], however, they cannot be used in the reported forms because they refer only to the high-Rayleigh number, or the convection dominated regime ($Nu \gtrsim 2$). More appropriate for the present geometric optimization problem is a Nu function that covers smoothly the entire range of possibilities, from conduction (small t_a) to convection (large t_a).

The solution we chose is based on the summary presented in [8, Fig. 5.8], which shows that the most frequently used high-Ra correlations are represented well by the analytical expression derived based on boundary layer theory [8,24]

$$Nu = 0.364\frac{t_a}{H}Ra_{H,\theta}^{1/4} \quad (\text{when } Nu \gtrsim 2). \tag{17}$$

It is worth pointing out that Eq. (17) is consistent with the pure conduction criterion (5); in other words, Eq. (17) holds when Eq. (5) fails. Next, we joined the high-Ra asymptote (17) with the pure conduction asymptote ($Nu = 1$) by using the technique of Churchill and Usagi [25]

$$Nu = \left[1 + \left(0.364\frac{t_a}{H}Ra_{H,\theta}^{1/4}\right)^m\right]^{1/m}. \tag{18}$$

For the curve-smoothing exponent we chose $m = 3$, which is an order of magnitude that has been used be-

fore (e.g., [26,27]). In summary, the overall resistance formula (15) can be nondimensionalized by using as reference scale the resistance across a completely solid wall $[L/(k_bHW)]$, and converting $Ra_{H,\theta}$ into $Ra_{H,\Delta T}$ via Eqs. (6) and (7)

$$\tilde{R} = \frac{R}{L/(k_bHW)} = \frac{k_b}{k_a}\phi\left[1+\left(0.364n^{-5/4}\phi\frac{L}{H}Ra_{H,\Delta T}^{1/4}\right)^m\right]^{-1/m} + 1 - \phi. \tag{19}$$

The overall resistance $\tilde{R}$ emerges as a function of the variable geometric parameters n and ϕ, and the fixed parameters k_b/k_a and the global parameter

$$b = \frac{L}{H}Ra_{H,\Delta T}^{1/4}. \tag{20}$$

The geometric parameters n and ϕ are related through the global stiffness constraint ($\tilde{I}$ = constant) displayed in Fig. 3.

In conclusion, when the stiffness constraint is invoked, the global resistance $\tilde{R}$ depends on only one geometric parameter, ϕ or n. This effect is illustrated in Fig. 4, which shows that $\tilde{R}$ can be maximized with respect to the number of air cavities. The $\tilde{R}$ maximum shifts toward larger n values (more numerous and narrower air gaps) as b increases. The $\tilde{R}$ maximization illustrated in Fig. 4 was repeated for other $\tilde{I}$ values in the range 0.7–0.95.

Let $\tilde{R}_{max}$ and n_{opt} denote the coordinates of the peak of one of the b = constant curves plotted in Fig. 4. The maximum resistance $\tilde{R}_{max}(b,\tilde{I})$ deduced from Fig. 4 and from similar calculations for other $\tilde{I}$ values, is reported in Fig. 5. Larger b values represent stronger natural convection, and this is reflected in smaller $\tilde{R}_{max}$ values. Larger $\tilde{I}$ values represent stiffer walls that use more solid material (Fig. 3), and, consequently, $\tilde{R}_{max}$ decreases as $\tilde{I}$ increases.

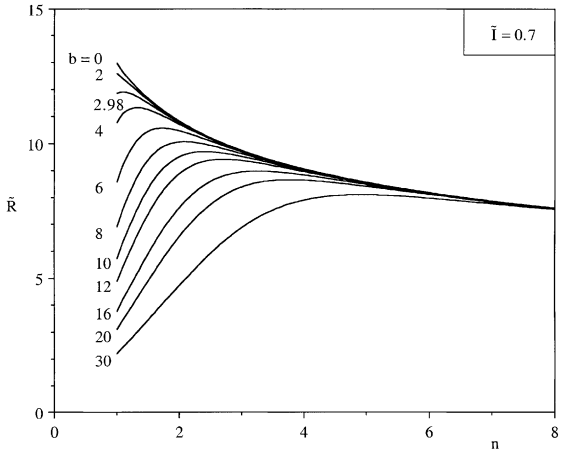

Fig. 4. The overall thermal resistance as a function of the number of air gaps when the external parameters b and $\tilde{I}$ are fixed.

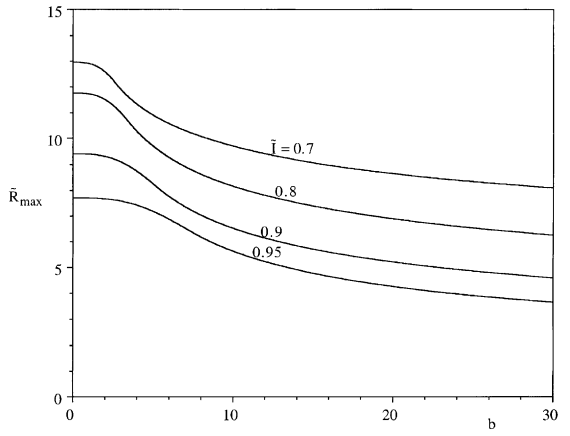

Fig. 5. The maximized wall thermal resistance as a function of the global natural convection parameter b and the global stiffness parameter $\tilde{I}$.

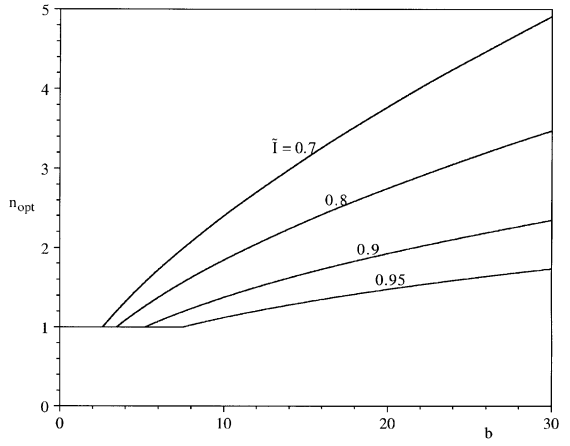

Fig. 6. The optimal number of air gaps as a function of the global natural convection parameter b and the global stiffness parameter $\tilde{I}$.

The optimal number of air gaps (n_{opt}) that corresponds to the $\tilde{R}_{max}$ results of Fig. 5 is reported in Fig. 6. Fewer air gaps are better when the natural convection effect is weak (small b), and when the required stiffness approaches that of the solid wall ($\tilde{I} = 1$).

The corresponding volume fractions of air and solid material can be calculated by combining Fig. 6 with Fig. 3. The result is the function $\phi(b,\tilde{I})$ reported in Fig. 7.

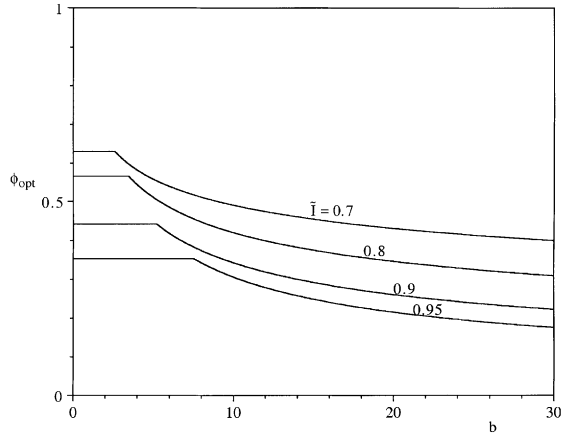

Fig. 7. The optimal air volume fraction as a function of the global natural convection parameter b and the global stiffness parameter $\tilde{I}$.

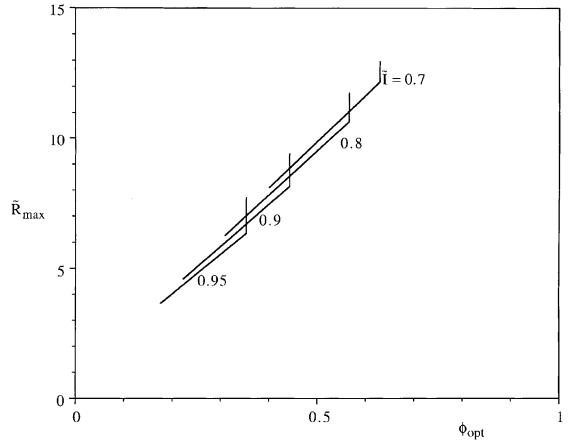

Fig. 8. The maximized thermal resistance versus the required air volume fraction when the overall stiffness is constrained.

More solid material (a smaller ϕ) is needed when the wall must be stiffer (a larger $\tilde{I}$), and when the natural convection effect is stronger (a larger b).

The optimal trade-off between the thermal and mechanical functions of the cavernous wall is also visible in Fig. 8. This figure shows the maximized resistance $\tilde{R}_{max}$ as a function of the optimized air volume fraction ϕ and the stiffness parameter $\tilde{I}$. Fig. 8 was obtained by combining Figs. 5 and 7, and eliminating b.

5. Fixed amount of solid

An alternative approach to selecting the internal structure of the wall is to consider the amount of solid material (or weight) as a constraint. The weight constraint replaces the stiffness constraint used in the preceding analysis. The fixed amount of solid material is such that when there are no cavities the wall thickness is L_0. We contemplate the design of a cavernous structure (Fig. 1) with n vertical air gaps of thickness t_a each, sandwiched between $(n+1)$ solid slabs of thickness t_b,

$$t_b = \frac{L_0}{n+1}. \tag{21}$$

The overall thickness of the cavernous wall is greater than L_0,

$$L = nt_a + (n+1)t_b, \tag{22}$$

where n and t_a may be varied independently. These two parameters are the degrees of freedom of the structure.

The overall thermal resistance of the wall with internal cavities can be written based on Eq. (15), where $\tilde{R}$ is defined in Eq. (19),

$$\tilde{R} = \frac{k_b n t_a}{k_a L_0 Nu} + 1. \tag{23}$$

We are interested in the effect of t_a and n on $\tilde{R}$. In the limit $t_a \to 0$, the heat transfer across each air gap is by pure conduction, and Nu approaches 1,

$$\tilde{R} = \frac{k_b n t_a}{k_a L_0} + 1. \tag{24}$$

In this limit $\tilde{R}$ increases linearly with the product nt_a, suggesting that the use of more numerous and wider air gaps leads to a better design.

The opposite extreme is when t_a is large enough so that the heat transfer through the air spaces is by boundary layer natural convection, cf. Eq. (17). The global thermal resistance in this limit is

$$\tilde{R} = \frac{k_b H n^{5/4}}{(0.364) k_a L_0 Ra_{H,\Delta T}^{1/4}} + 1. \tag{25}$$

It shows that t_a no longer influences thermal performance when convection dominates in the air space, i.e., $\tilde{R}$ does not have a maximum with respect to t_a. In this limit $\tilde{R}$ continues to increase as the number of air slots increases, i.e., as the total thickness of the wall increases. The limits (24) and (25) are sketched in Fig. 9.

Eq. (25) represents the highest resistance that can be achieved by increasing t_a at constant n. To find the critical t_{ac} value that is 'large enough', we intersect the limits (24) and (25), as shown in Fig. 9,

$$t_{ac} \sim 3Hn^{1/4} Ra_{H,\Delta T}^{-1/4}. \tag{26}$$

Air spaces that are made thicker than this size will not contribute more to the overall thermal resistance of the wall.

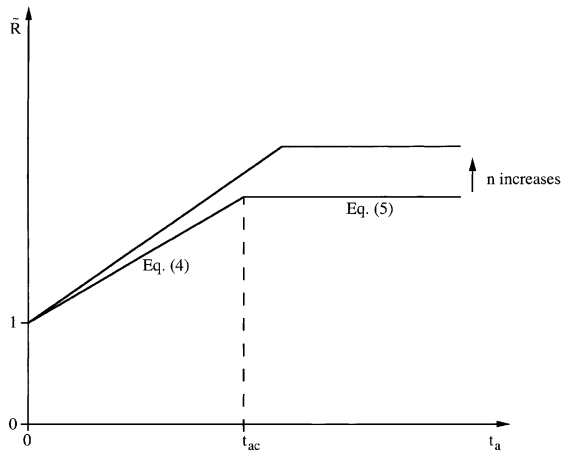

Fig. 9. The effect of the air gap thickness and the number of air gaps on the overall thermal resistance of a cavernous wall with fixed weight.

6. Concluding remarks

In this paper we showed that the internal structure of a cavernous wall can be derived optimally from the competition between the thermal insulation and mechanical strength functions of the wall. This combination of two functions, thermal and mechanical, is new in an optimization at such a simple and fundamental level. Previous studies of walls with air enclosures have dealt only with the thermal insulation characteristics of various wall structures.

In addition, the competition between the thermal and mechanical functions of the structure represents an extension of the method of constructal design – the generation of geometric form based on the maximization of global performance subject to global constraints. Most of the constructal design work that has been performed so far [3] was based on the maximization of heat and fluid flow performance in isolation, without reference to mechanical strength. Similarly, considerably older examples of constructal design are known in the field of strength of materials, where strength was maximized and configuration was optimized without reference to thermofluid performance (e.g., [11, p. 106]).

The simultaneous consideration of the thermal and mechanical functions of the complex structure is the defining feature of the problem proposed in this paper. We showed that the number of air gaps built into the wall can be optimized when the overall stiffness is specified. The optimal number of air gaps increases when the effect of natural convection increases, and when the specified wall stiffness decreases. The maximized wall thermal resistance is larger when the effect of natural convection in the air gaps is weaker, and when the wall stiffness is smaller. The optimal volume fraction occupied by air in the cavernous structure decreases when the natural convection effect becomes stronger, and when the wall stiffness increases.

This problem can be pursued from alternative points of view, depending on the objectives of the greater system to which the cavernous wall belongs. We took a step in this direction in Fig. 9, where we showed the relation between internal geometry and global thermal performance when the weight of the wall is fixed. Another possible direction is to frame the optimization on the basis of thermoeconomics [28–33], by attaching costs to the heat loss through the wall, and to the construction of the wall, and minimizing the total cost over the lifetime of the system. Thermoeconomics is a promising extension for future work not only on this problem but also in constructal design in general. For example, many of the engineered flow systems that in [3] derived their geometry from the optimal balancing of flow resistances, could have their architectures derived based on the minimization of total cost.

The combined 'flow and strength' geometric optimization method illustrated in this paper can be applied in other fields where mechanical structures must carry loads while posing least resistance to internal and external flows. Good candidates are the mechanical structures of aircraft, ships and automobiles. For example, it was shown that the cruising speeds of all flying bodies (aircraft, birds, insects) can be predicted approximately by minimizing the total flying power requirement, i.e., by focusing on fluid flow optimization (e.g., [3, pp. 234–240]). The deviations from these predictions may be accountable on the basis of mechanical strength considerations, in addition to and simultaneously with flow considerations. This combination may be carried further into the design of structural elements for vehicles, which, like the wall of Fig. 1, could be conceptualized and morphed into geometric forms with more than one function.

Acknowledgements

The work reported in this paper was supported in part by a grant from the National Science Foundation. The authors thank Mr. W. Wechsatol for assistance in the final stages of this paper.

References

[1] S. Lorente, Heat losses through building walls with closed, open and deformable cavities, Int. J. Energy Res. 26 (2002), to appear.

[2] B. Lartigue, S. Lorente, B. Bourret, Multicellular natural convection in a high aspect ratio cavity: experimental and numerical results, Int. J. Heat Mass Transfer 43 (2000) 3159–3170.

[3] A. Bejan, Shape and Structure, from Engineering to Nature, Cambridge University Press, Cambridge, UK, 2000.
[4] S. Kakac, W. Aung, R. Viskanta (Eds.), Natural Convection: Fundamentals and Applications, Hemisphere, Washington, DC, 1985.
[5] K.T. Yang, Natural convection in enclosures, in: S. Kakac, R.K. Shah, W. Aung (Eds.), Handbook of Single Phase Convective Heat Transfer, Wiley, New York, 1987, Chapter 13.
[6] B. Gebhart, Y. Jaluria, R.L. Mahajan, B. Sammakia, Buoyancy-Induced Flows and Transport, Hemisphere, New York, 1988.
[7] Y. Jaluria, Natural Convection Heat and Mass Transfer, Pergamon, Oxford, UK, 1980.
[8] A. Bejan, Convection Heat Transfer, 2nd ed., Wiley, New York, 1995.
[9] A. Bejan, A synthesis of analytical results for natural convection heat transfer across rectangular enclosures, Int. J. Heat Mass Transfer 23 (1980) 723–726.
[10] R.L. Frederick, On the aspect ratio for which the heat transfer in differentially heated cavities is maximum, Int. Commun. Heat Mass Transfer 26 (1999) 549–558.
[11] J.P.D. Hartog, Strength of Materials, Dover, New York, 1961.
[12] F.P. Beer, E.R. Johnston Jr., J.T. DeWolf, Mechanics of Materials, 3rd ed., McGraw-Hill, Boston, 2002.
[13] F. Landis, A. Rubel, Discussion of Ref. 14, J. Heat Transfer 92 (1970) 167–168.
[14] M.E. Newell, F.W. Schmidt, Heat transfer by natural convection within rectangular enclosures, J. Heat Transfer 92 (1970) 159–167.
[15] D.W. Pepper, S.D. Harris, Numerical simulation of natural convection in closed containers by a fully implicit method, J. Fluids Eng. 99 (1977) 649–656.
[16] G. de Vahl Davis, Laminar natural convection in an enclosed rectangular cavity, Int. J. Heat Mass Transfer 11 (1968) 1675–1693.
[17] A.F. Emery, The effect of a magnetic field upon the free convection in a conducting fluid, J. Heat Transfer 85 (1963) 119–124.
[18] J.J. Portier, O.A. Arnas, Heat Transfer and Turbulent Buoyant Convection, vol. II, Hemisphere, Washington, DC, 1977.
[19] G. Burnay, J. Hannay, J. Portier, Heat Transfer and Turbulent Buoyant Convection, vol. II, Hemisphere, Washington, DC, 1977.
[20] A. Rubel, R. Landis, Numerical study of natural convection in a vertical rectangular enclosure, Phys. Fluids 12-II (1969) 208–213.
[21] C. Quon, High Rayleigh number convection in an enclosure: A numerical study, Phys. Fluids 15-I (1972) 12–19.
[22] J.E. Fromm, A numerical method for computing the nonlinear, time dependent, buoyant circulation of air in rooms, in: Building Science Series No. 39, National Bureau of Standards, Washington, DC, 1971.
[23] A. Gadgil, F. Bauman, R. Kammerud, Natural convection in passive solar buildings: experiments analysis and results, Passive Solar J. 1 (1982) 28–40.
[24] A. Bejan, Note on Gill's solution for free convection in a vertical enclosure, J. Fluid Mech. 90 (1979) 561–568.
[25] S.W. Churchill, R. Usagi, A standardized procedure for the production of correlations in the form of a common empirical equation, Indust. Eng. Chem. Fund. 13 (1974) 39–46.
[26] A. Bar-Cohen, W.M. Rohsenow, Thermally optimum spacing of vertical natural convection cooled parallel plates, J. Heat Transfer 106 (1984) 116–123.
[27] M. Wang, A. Bejan, Heat transfer correlation for Bénard convection in a fluid saturated porous layer, Int. Commun. Heat Mass Transfer 14 (1987) 617–626.
[28] S.S. Stecco, M.J. Moran, Energy for the Transition Age, Nova Science, New York, 1992.
[29] H.J. Richter (Ed.), Thermodynamics and the Design, Analysis and Improvement of Energy Systems 1993, HTD-vol. 266, ASME, New York, 1993.
[30] R.J. Krane (Ed.), Thermodynamics and the Design Analysis and Improvement of Energy Systems 1994, AES-vol. 33, ASME, New York, 1994.
[31] R.J. Krane (Ed.), Thermodynamics and the Design, Analysis, and Improvement of Energy Systems 1995, AES-vol. 35, ASME, New York, 1995.
[32] A. Lazzaretto, G. Tsatsaronis, On the quest for objective equations in energy costing, in: M.L. Ramalingam, J.L. Lage, V.C. Mei, J.N. Chapman (Eds.), Proceedings of the ASME Advanced Energy Systems Division, AES-vol. 37, 1997, pp. 197–210.
[33] A. Bejan, G. Tsatsaronis, M. Moran, Thermal Design and Optimization, Wiley, New York, 1996.